RSC Advances

REVIEW

View Article Online
View Journal | View Issue

Cite this: *RSC Adv.*, 2023, **13**, 16145

A brief review: the application of long afterglow luminescent materials in environmental remediation

Yuxin Guo, * Qiuwen Wang, Siyu Liu, Wen Ya, Ping Qi, Zenan Ni,* Huimin Liu and Qijian Zhang

Received 29th March 2023
Accepted 2nd May 2023

DOI: 10.1039/d3ra02046k

rsc.li/rsc-advances

Long afterglow luminescent (LAL) materials can release their stored light after turning off the light irradiating on them. Because of this unique characteristic, the coupling of LAL materials and conventional semiconductors is an environmental-friendly method for supporting photocatalytic activity for environmental remediation. Currently, the exploration of "afterglow-catalysis" materials for the fabrication of around-the-clock photocatalytic systems is still in its infancy. Accordingly, herein, we summarize the application of LAL materials in photocatalytic environmental remediation and energy crisis alleviation to stimulate further motivation for the development of novel LAL materials. By discussing the works in the last five years on novel LAL materials, we anticipate the development of new materials, *i.e.*, "afterglow-catalysis" composites, to realize waste-to-energy, even achieving industrialization.

1 Introduction

Currently, modern society has witnessed rapid development, which is accompanied by an environmental crisis, having a severe effect on the ecosystem.[1,2] Given that fossil fuels and water sources have been overexploited for industrial growth, the excess emission of CO_2 and contamination of water, especially from the textile and printing industries, have drawn attention globally.[3,4] Furthermore, the release of heavy metal ions (HMIs),[5,6] organic toxic pollutants[7] and industrial waste air/water has resulted in global warming and abnormal climatic changes.[8,9] Thus, to address this situation, hundreds of thousands of scientists have devoted their efforts to finding better strategies.[10–12]

Among the reported strategies, photocatalytic technology has emerged as one of the most prospective alternative methods for the utilization of sunlight. Photocatalysis is a sustainable green technology, which is internationally recognized as an ideal strategy. Suitable semiconductor-based photocatalysts can oxidize and decompose various toxic compounds to purify ecosystems; meanwhile, photocatalysts are competitive candidates for the CO_2/NO_x reduction reaction.[13,14] Photocatalysis is a promising method involving non-spontaneous strong oxidation processes. As its name implies, photocatalysis requires a steady light source to maintain the reaction. Nevertheless, due to the alternation of day and night due to the rotation of the Earth, sunlight cannot meet the requirements of round-the-clock photocatalysis, which is one of the main problems that limit the industrial application of photocatalytic technology.[15–17] Thus, to address this limitation, new types of materials or methods to overcome the drawback of the initiation source need to be developed.

In recent years, long afterglow luminescent (LAL) materials have shown unique advantages in the field of photocatalysis, owing to their special mechanism of photoelectron storage and release. LAL materials have witnessed rapid headway in research and development.[18,19] LAL materials are special photocatalytic materials, which are also called persistent luminescent materials. LAL is a particular optical phenomenon in which a material keeps emitting in the UV, Vis or IR spectral regions for several minutes, hours or even days after the excitation stops.[20] Thus, long afterglow luminescence is considered a suitable inner light source for photocatalysts. Consequently, self-induced photocatalytic activity can be continuously generated when the external irradiation source is turned off. A novel material was constructed by combining an LAL material and semiconductor-based photocatalyst, which could prolong the operation of photocatalysis around the clock. This type of material can solve the abovementioned restrictions, which is called afterglow-catalyst. The various modification strategies to construct afterglow-catalyst systems include heterojunction construction, surface modification and defect engineering. In afterglow-catalyst systems, two important issues should be considered, *i.e.*, traps and adsorptive/catalytic sites. The effective traps are related to the charge storage capacity, which shows the capability of storing/releasing photoexcitation energy.[21] Adsorptive/catalytic sites act as catalytic sites, which are essential for the design of afterglow-catalysts.[22]

School of Chemical and Environmental Engineering, Liaoning University of Technology, Jinzhou, 121001, China

2 Mechanism

The phenomenon of LAL is complicated, and thus research has been conducted for decades to understand it. To achieve a deeper understanding of the application of LAL materials in photocatalysis, here we introduce the general concept of long persistence luminescence.[17] The mechanism of LAL is related to four parts, as follows: (a) excitation of charged carriers. Upon effective optical charging (UV, Vis or IR light), electronic implantation (electron beams) or high energy-ray irradiation (X-ray, beta ray or gamma radiation), charge carriers (electrons or holes) are generated, with the delocalization and migration of charge carriers. (b) Storge of charged carriers. The excited carriers are firmly captured on the trapping states, while the storage capacity of the trapping states strongly depends on the types and numbers of carriers and defects. (c) Release of charged carriers. Captured carriers escape from the traps. In addition to the depths of the traps in the hosts, the release rate of carriers captured in the traps can also be influenced by the disturbance in the external field (thermal, optical or mechanical disturbance), enabling control of the persistent luminescence duration. (d) Recombination process of charged carriers.[18]

At present, although charge carrier traps play a key role in all the suggested afterglow descriptions, the mechanism of electron retention in long afterglow luminescence is still controversial, which can be found in some previously published works.[18,23,24] In this section, we briefly introduce the commonly accepted mechanism based on the conduction band- or valence band-involved processes.

Generally, Matsuzawa *et al.* reported the origins of extraordinary persistent luminescence and assumed that holes are the main charge carriers, which has been widely accepted. This assumption was also proven by Abbruscato *et al.* based on their earlier measurements on non-co-doped $SrAl_2O_4$:Eu^{2+}, which showed a weak LAL phenomenon, suggesting that the holes in the valence band were the main charge carriers.[25,26] Matsuzawa *et al.* further explained that when Eu^{2+} is excited by a photon, a hole escapes to the VB, thereby leaving behind Eu^{+}. Subsequently, the hole is captured by a trivalent rare earth ion such as Dy^{3+}, thus creating Dy^{4+}. Eu^{2+} and Dy^{3+} are the electron trapping center and hole trapping center, respectively. Thereafter, the captured hole can be released *via* thermal energy into the valence band again, travelling back to Eu^{+}, with a photon emitting energy. Fig. 1(a) shows the mechanism of the Matsuzawa model based on $SrAl_2O_4$:Eu^{2+}, Dy^{3+}.

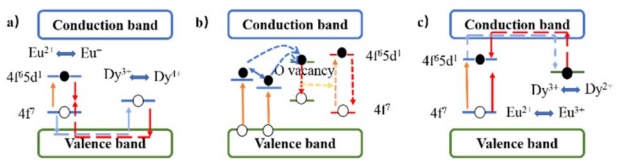

Fig. 1 Schematic diagram of the Matsuzawa model based on $SrAl_2O_4$:Eu^{2+}, Dy^{3+} (a), energy transfer model based on $CaAl_2O_4$:Eu^{2+}, Dy^{3+} (b) and electron trapping model based on aluminate and silicate (c). (Reproduced from ref. 25 with permission from Chinese Laser Press, Copyright 2021).

Aitasalo *et al.* proposed that direct transitions are excited from the valence band into unspecified traps because the energy level of the CB is much higher than that of the oxygen vacancy traps, making it impossible for a transition to CB assisted by a thermal process.[27] They proposed that the energy released on recombination of the hole and electron is utilized by the Eu ions directly. Trivalent rare earth ions and co-dopants increase the number of lattice defects in the electron model because the divalent alkaline earth sites are occupied by lattice defects, and spontaneous defects are used to compensate for the charge.[28] However, they disagreed that the Eu^{+} or Dy^{4+} ions in oxide compounds at room temperature are unstable ions in the redox reaction. Fig. 1(b) shows the mechanism of the energy transfer model based on $CaAl_2O_4$:Eu^{2+}, Dy^{3+}.

Dorenbos *et al.* revised the electron model after Aitasalo *et al.*, which was called the energy band engineering model. They assumed that the electrons were excited from Eu^{2+} rather than the valence band.[29,30] Given that the 5d level of Eu^{2+} is close to the conduction band, the excited electrons can easily enter the conduction band, and then be captured by the trivalent rare earth ions. Upon thermal treatment again, the captured electrons are released to the conduction band, accompanied with their recombination and release from the $4f^7$ level to the $5d^1$ state, thereby causing the release of photon energy. Fig. 1(c) shows the mechanism of the electron trapping model based on aluminate and silicate.

Besides the conduction band-valence band model, the oxygen vacancy model and quantum tunneling model are widely accepted models, although it is difficult to explain all the phenomena of LAL using these mechanisms. The study of the mechanism of LAL not only predicts the types of carriers during electron capture and release, but also reveals the mechanism of action of the afterglow luminescence center.

3 Application

In recent years, several photocatalysts have been applied to address environmental remediation, including the degradation of dyes and removal of toxic air. Afterglow-catalysis, as a key interest in the field of photocatalysis currently, is related to technology trends. As its name suggests, photocatalytic reactions need an appropriate light source, which can sustain photocatalytic activity. However, once irradiation, ceases, photocatalysts are deactivated. Thus, sustaining a light source is a necessity for photocatalysis. Besides a light source, a wide bandgap semiconductor is another crucial component in the entire process. Conventionally, commercial semiconductors such as TiO_2 (3.2 eV), ZnO (3.37 eV) and g-C_3N_4 (2.7–2.8 eV) are widely used as photocatalysts, which have low band gap values, excellent photostability and low electron–hole recombination.[31] If semiconductors are excited with photo energy equivalent to or greater than their band gap to generate electron–hole pairs, they can act as photocatalysts, which drive reactions on their surface.[32] In this part, the representative reports in the last five years on the application of LAL materials in environmental remediation are summarized.

3.1 Degradation of organic dyes

Currently, the demand of environmental remediation has grown dramatically, especially, considering the huge amount of organic dyes consumed each year, destroying the ecological balance globally. Organic dyes, such as methylene blue (MB), methyl orange (MO) and rhodamine B (RhB) pose a serious threat to aquatic species and human health, and thus the degradation of organic dyes has been investigated to alleviate environmental problems in recent years. Nowadays, several methods have been developed to achieve this, including physical adsorption, electron coagulation, membrane filtration, reverse osmosis, and biochemical process.[33,34] The photocatalytic process involves the oxidation of organic dyes with the help of sunlight or artificial light and no by-products are generated, avoiding the need for further purification. These advantages of photocatalytic technology in wastewater purification have attracted significant attention.

TiO_2 is the chief candidate in the photocatalytic field. Furthermore, to enhance its photocatalytic activity, TiO_2 is modified by doping non-metal ions and metal ions, which is a commonly adopted method. Another way to promote the photocatalytic activity of TiO_2 is by assembling it with LAL materials, which can be used under dark conditions. Fan *et al.* reported the modification of TiO_2 with three types of metal ions, including Cr, Co and Ni (M-TiO_2). Subsequently, (M-TiO_2) was combined with $MgAl_2O_4$:(Pr^{3+}, Dy^{3+}), which stored energy and emitted an emission at the wavelength of 562 nm.[35] M-TiO_2 absorbed the light energy from $MgAl_2O_4$:(Pr^{3+}, Dy^{3+}) to sustain photocatalytic activity for the degradation of MO, where $MgAl_2O_4$:(Pr^{3+}, Dy^{3+})/M-TiO_2 exhibited the great efficiency of 71.8% degradation.

In the work reported by Vaiano, nitrogen-doped TiO_2 (N-TiO_2) was synthesized *via* the sol–gel method as a catalyst, which was associated with commercial long afterglow blue phosphors (SrSiP) to treat contaminated water using UV-LED irradiation.[36] After 30 min illumination from UV-LEDs, CV was faded, validating that this photocatalyst can be applied in wastewater treatment. SrSiP phosphors can store electrons and release them slowly when UV light illumination is ceased, where the use of N-TiO_2/SrSiP to achieve this is important from an economic perspective, given that it can save about 42% energy. It is worthwhile to note that this paper was the first to report a reduction in electricity usage with the use of a photocatalyst and SrSiP excited by LEDs.

In Ma's study, a commercial TiO_2 photocatalyst was coated on solid-state $BaZrO_3$ derivates *via* a sol–gel process.[37] The emission spectrum of Mg-doped $BaZrO_3$ overlapped partly with the absorption spectrum of TiO_2. This result indicated that the $BaZrO_3$-doped 1.5 mol% Mg^{2+} acted as an assistant excitation source for the commercial photocatalyst TiO_2, which can decompose MB in the dark. In a solution of MB containing $BaZrO_3$: Mg^{2+}/TiO_2 composite after UV irradiation, the decomposition rate approached 10% after 12 min, and the researchers conducted a control experimental, showing that Mg^{2+} enhanced the violet-blue long afterglow to support photocatalytic activity in the dark.

Zhou *et al.* also used $CaAl_2O_4$:Eu^{2+}, Nd^{3+} (CAOED), emitting blue luminescence with a maximum intensity at 450 nm. The luminescence intensity of CAOED can excite g-C_3N_4, and therefore CAOED-coupled g-C_3N_4 QDs exhibited photocatalytic activity for the degradation of MO, with its effectiveness lasting for over 3 h at night and returning to the initial state after the reaction.[38] This paper proved that the ideal photocatalyst released electrons gradually from CAOED, which can excite g-C_3N_4 QDs. The electrons were transferred through the surface of g-C_3N_4 QDs and reacted with water and oxygen to generate ROS species, with the hole oxidation process resulting in the photodegradation of MO.

Fan *et al.* aimed to investigated the light source of the photocatalytic reaction, which is necessary to stimulate photocatalytic reactions.[39] They offered a strategy of combining g-C_3N_4 with $SrAl_2O_4$:Eu^{2+}, Dy^{3+} (SAO) to obtain a photocatalyst that is not dependent on a continuous source of solar or artificial light. $SrAl_2O_4$:Eu^{2+}, Dy^{3+} (SAO)-driven g-C_3N_4 exhibited an excellent catalytic performance for the degradation of MO, where the concentration of MO decreased rapidly after reaching adsorption equilibrium, and the photocatalyst was stable. More importantly, g-C_3N_4/$SrAl_2O_4$:Eu^{2+}, Dy^{3+} (SAO) exhibited an excellent photocatalytic performance in actual water under either sunlight or dark conditions. This work provides a strategy for constructing photocatalysts to address the serious water pollution problem, thus promoting their application in the field of environmental pollution.

Chen's group synthesized a binary composite, *i.e.*, SAO/g-C_3N_4 ($SrAl_2O_4$:Eu^{2+}, Dy^{3+}/g-C_3N_4), through high-temperature calcination, which was used for the photodegradation of water pollutants.[40] This new composite catalyst exhibited an excellent degradation performance using basic fuchsin (BF) as the substrate, where the degradation ratio of BF reached 100% in 30 min under light illumination. When the external electrical source was removed, the long afterglow phosphors SAO could act as a light source to degrade BF at night or on a cloudy day, achieving a degradation efficiency of over 90% in 3 h. During the degradation process, the $^{\bullet}O_2^-$ radical played an active role and ESR captured the $^{\bullet}O_2^-$ radical in the experiment as further verification.

Besides metal element loading on the surface of SMS, g-C_3N_4, as a metal-free polymeric, exhibits advantages in the field of photocatalysis due to its narrow band gap (2.8 eV). Hong *et al.* synthesized SAED/g-C_3N_4 by synthesizing a g-C_3N_4 and phosphorescent material ($Sr_{0.95}Eu_{0.02}Dy_{0.03}Al_2O_4$, SAED) composite *via* the thermal oxidation method.[41] The photocatalytic efficiency of SAED/g-C_3N_4 was analyzed for the photodegradation of organic pollutants, such as MB, MO and RhB, and compared with g-C_3N_4. In the absence of light, the results showed that the decomposition of organic pollutants was higher than pristine g-C_3N_4 due to phosphorescence. Phosphorescence as the light source was supported to degrade organic pollutants by SAED in the dark, and this phenomenon was explained by the decline in the recombination rate of electrons and holes, resulting in prolonged phosphorescence.

$ZnGa_2O_4$ is not only an excellent photoluminescence host for blue-emitting phosphors but also an excellent photocatalyst

with a wide band gap. When another ion was doped in $ZnGa_2O_4$, the intensity of LAL materials enhanced significantly. Turdi *et al.* synthesized a dual-functional LAL material with photocatalytic activity base on $ZnGa_2O_4$ *via* a facile one-step method, which was less than 10 nm in size, co-doping Bi^{3+} and Cr^{3+}.[42] $ZnGa_2O_4$ played a crucial role in the photo-catalyst owing to its *Fd3m* space group; meanwhile, the hybridized orbitals and band gap benefitted the electron mobility and absorption of UV light efficiently.[43–45] Co-doped Bi^{3+} and Cr^{3+} of $ZnGa_2O_4$ exhibited excellent dual-functional with the NIR emission band peaking at 698 nm and photo-degradation of RhB. The authors confirmed that the holes were the main species in the photoreaction of RhB, compared with ROS.

Zhang's group etched Cr^{3+}-doped $ZnGa_2O_4$ by EDTA to get ZGO-EDTA, which generated more oxygen vacancies on its surface, with the goal of accumulating visible light to activate afterglow.[22] The generated oxygen vacancies on the surface of ZGO-EDTA slowed down the recombination of photocarriers and extended the length of the afterglow. The efficiency of photodegradation was measured by common organic pollutants such as MB, MG and CV. ZGO-EDTA showed the degradation rate of MB of 93.4% at 24 h, suggesting that doped-Cr^{3+} played the dominant role in the photodegradation reaction in the dark as the light source. They provided possibilities for performing photocatalytic reactions whenever and wherever desired and widen their application prospect.

A highly productive and reusable catalyst was developed for the photodegradation of organic pollutants in aqueous solution by Menon.[46] The combination of $SrAl_2O_4$:Eu^{2+}, Dy^{3+} (SAO) and ZnO almost degraded MO under UV-irradiation in 1 h, where the excellent performance of the photocatalyst resulted from the synergistic effects between the persistent luminescent phosphor $SrAl_2O_4$:Eu^{2+}, Dy^{3+} (SAO) and ZnO. The mechanism of $SrAl_2O_4$:Eu^{2+}, Dy^{3+}@ZnO (SAZ) is illustrated in Fig. 2, where the photocatalytic mechanism of SAZ is based on the Matsuzawa model, with hole–electron pair migration occurring between SAO and ZnO. When electrons were created by the light source, exciting Eu^{2+} from the ground state, they were captured by the Eu^{2+} excited state to get Eu^{+}, and holes were created on the SAO VB. Some of the holes migrated to the ZnO VB and participated in photocatalytic reaction, where a small amount of holes transferred to Dy^{3+}, which modified Dy^{4+}, leaving behind deep-level traps. After the external irradiation was removed, no new holes were generated, and e-h recombination occurred.

Silver-based photocatalysts with a small band gap are easily activated by visible light, particularly loading Ag on the surface improves the light adsorption and photogeneration of electrons and holes. Hai *et al.* used decorated Ag/$Sr_2MgSi_2O_7$:Eu^{2+}, Dy^{3+}(SMS) as a photocatalyst with unique carrier transport paths and large number of crystal defects, where Ag was introduced in the LAL material for enhancing its performance.[47] Under UV irradiation, the decomposition rate of RhB was 45.1% by Ag/SMS, and the degradation rate of RhB reached 76.5% after 24 h in the dark, with the final degradation rate as high as 88.9%. The reason for the efficient photocatalytic degradation was that Ag interfaced on the SMS with a suitable bandgap can enable the separation of electrons and holes. Fig. 3 shows the energy level and photogenerated carrier path diagram of $Sr_2MgSi_2O_7$:Eu^{2+}, Dy^{3+}. Ag/SMS achieved around-the-clock photocatalysis due to the carriers stored in the traps, which continued to be released slowly and transferred to participate in the reaction, enabling the photocatalysis reaction to proceed in the dark.

The $Sr_2MgSi_2O_7$:Eu^{2+}, Dy^{3+}/Ag_3PO_4(SMSED/APO) composite as a cubic porous material was combined through an *in situ* growth method by Wang's group.[48] The degradation effect of SMSED/APO was tested by using degradation rate of three different organic dyes under UV light and at night, where among them, the degradation of RhB was the fastest, which was ascribed to the pore structure energy-saving assisting photodegradation, achieving 80% degradation efficiency through 1/3 APO, and SMSED/APO could be recycled several times. APO possesses good catalytic effects, which was proven by its electron–hole separation rate, and APO was incorporated with $Sr_2MgSi_2O_7$:Eu^{2+}, Dy^{3+} to lengthen the photocatalytic time as a round-the clock light source to excite the photocatalytic reactions, no longer depending on light conditions. Their work provides a new idea for preparing photocatalytic composite materials.

In the same year, Zhang *et al.* reported the preparation of another novel afterglow-catalysis system, which was developed

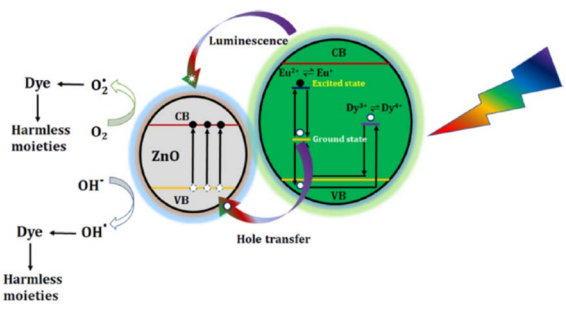

Fig. 2 Schematic diagram of photocatalytic mechanism SAZ based on electron–hole model (reproduced from ref. 46 with permission from Elsevier, Copyright 2021).

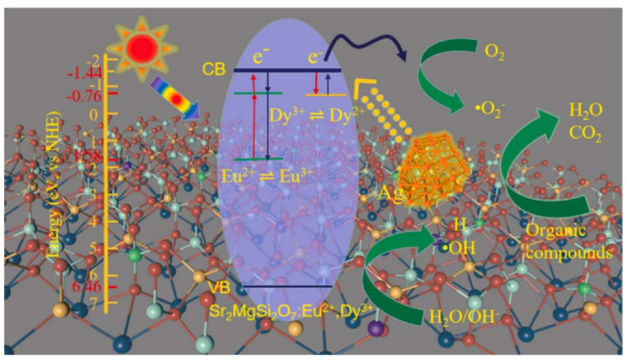

Fig. 3 Energy-level and photogenerated electron transfer process diagram of Ag/SMS and schematic of its photocatalytic reaction. (Reproduced from ref. 47 with permission from Elsevier, Copyright 2021.)

using $CaAl_2O_4$:Eu^{2+}, Nd^{3+} as the illuminant and Ag_3PO_4 as the photocatalyst. It degraded RhB in water effectively, where the degradation rate was improved by depositing nano-Pt on the surface of Ag_3PO_4.[49] The enhanced performance for the degradation of RhB was illustrated by afterglow-catalytic mechanism, where the nano-Pt particles can capture and store photoelectrons from Ag_3PO_4 because the energy level of the CB is more positive than the Fermi energy of Pt, the electrons readily shifted from the CB of Ag_3PO_4 to nano-Pt, and Pt performed the preferable role of capturing and storing electrons, serving as an electron divertor.[50] Taken together, Ag_3PO_4 exhibited excellent photooxidative activity, where its separation efficiency of photogenerated electrons and holes lay the groundwork for absorbing light to decompose organic pollutants.

Zhang *et al.* devoted their efforts to the practical application of materials in environmental remediation. Based on their previous works on photocatalysts in environmental remediation,[51,52] they proposed an environmentally friendly three-dimensional (3D) network structure photocatalyst for the degradation organic dyes.[53] The novel 3D hydrogel structure was composed of chitosan, graphene oxide and zinc oxide, which has large specific surface area and porous structure, which blocked the direct contact between ZnO and water, and thus the dissolution of Zn^{2+} ions was alleviated and the effect of photo-corrosion on catalytic activity was reduced to improve the photo-corrosion-resistance of traditional ZnO. The efficient photodegradation rate was up to 96.5% for MB and 92.2% for RhB. The stable and recycled hydrogel material provides enlightenment for removing organic pollutants.

To enhance the ability of photocatalysts to absorb visible light, core@shell structures act as a surface-modified method to make them responsive to visible light and alleviate the possible chemical corrosion.[54] Hsu's group reported the synthesis of Au@Cu_2O core@shell nanocrystals, which can control shell thicknesses and continuously operate under illumination and darkness for the efficient degradation for MB and *E. coli*.[55] In their work, the Au core was protected by the shell from aggregating during the reaction period; furthermore, by embedding Au in the shell, the chance of corrosion of Au was alleviated, and thus the life of the photocatalyst could be extended and long-term catalytic operation could be realized. Cu^+ and Fe^{2+} can catalyze $^{\cdot}OH$ radicals in the presence of H_2O_2, which is an effective substance for degrading organic pollutants. Their findings represent a practical strategy for building novel catalyst systems for environmental remediation.

In the past five years, several researchers investigated different LAL materials combined with semiconductor photocatalysts to decompose organic dyes. The innovative afterglow-catalytic system showed excellent photocatalytic activity for organic pollutant degradation not only under irradiation but also in the power off condition. Thus, afterglow-catalytic systems have been very popular and significant progress has been gained, with great efforts still in progress. Here, for convenience, the above-mentioned studies are listed in Table 1.

3.2 Removal of NO

Environmental remediation not only involves the removal of organic dyes in aquatic bodies, but also the accumulated anthropogenic atmospheric pollutants in the urban atmosphere, as the prime hotspot for society. With the booming industrial development, adequate poisonous atmospheric materials such as nitrogen oxides (NO_x) from automobile exhausts and fossil fuels have a negative effect on human health, and thus it is necessary to remove NO_x gases from the urban atmosphere. Research on the removal of NO_x (De-NO_x) has progressed in the past few decades. Accordingly, pre-combustion, combustion and post combustion technology has improved, where most of the methods used are chemical and physical processes. However, they have several disadvantages, limiting their large-scale applications such as high temperature and high concentration. In survey of the curve of NO_x content with time during the day,[56] the changing trends of NO_x content showed that the NO_x concentration decreased in the daylight and steeply rise from 19–24 h. This suggests that sunlight helps in the photocatalytic removal of NO_x, and the necessity of developing photocatalysts has increased with the aim to degrade NO_x. Air pollutants can be decomposed by photocatalytic reaction with the assistance of illuminants, and consequently a suitable excitation light is an essential part to stimulate the photocatalytic process. In this case, long persistent materials can store energy and release energy to stimulate photocatalytic reactions as an *in situ* light source after removal of the excitation light source. Therefore, combining long persistent materials with photocatalysts has attracted interest from researchers interests in this research field recently.

In previous studies, g-C_3N_4 was reported to have potential for environmental remediation due to its abundance, low cost, chemical stability, narrow bandgap (2.7 eV) and simple preparation process.[19,57,58] g-C_3N_4 is also widely used for the removal of NO, which has a low band gap value, excellent photostability and low electron–hole recombination efficiency.[18] To the best of our knowledge, T. Sato's research group investigated the removal of NO_x after combustion in the dark. Besides coating, surface deposition and physical mixing are common ways to couple LAL materials with photocatalytic materials to construct new systems to explore the De-NO_x processes.[59]

Yang's group proposed that LAL materials can be stimulated in the photochemical process *in situ* as an internal light source, and thus g-C_3N_4/$Sr_2MgSi_2O_7$:(Eu, Dy) was prepared *via* a thermal polymerization method. It achieved a good effect on the removal NO_x, where the emission spectrum of $Sr_2MgSi_2O_7$:(Eu, Dy) is in the range of 420–600 nm, which matched the absorption region of g-C_3N_4 for the construction light-storage-assisted photocatalysts.[60]

In 2021, they used urea to prepare g-C_3N_4, and then attached it to $Sr_2MgSi_2O_7$:(Eu, Dy) with different mass ratios to obtain composites.[56] The photocatalytic performance of the coupled g-C_3N_4 with $Sr_2MgSi_2O_7$:(Eu, Dy) was verified by the removal NO as a pollutant, and the highest NO removal efficiency was 70.73% with a mass ratio of 2 : 1, and the composite not only had the best removal efficiency of NO under a light source, but

Table 1 Long afterglow luminescent materials with semiconductors for the removal of photocatalytic organic pollutants

Long afterglow luminescent materials and composites	Emission wavelength/range (nm)	Pollutants	Degradation efficiency and time	Reference
SrSiP, N-TiO_2	440 nm	CV	40% in 180 min	36
Mg-$BaZrO_3$, TiO_2	410 nm	MB	10% in 12 min	37
$CaAl_2O_4$:Eu^{2+}, Nd^{3+}, g-C_3N_4	465 nm	MO	56.9% in 120 min	38
$SrAl_2O_4$:Eu^{2+}, Dy^{3+}, g-C_3N_4	—	BF	90% in 3 h	40
$ZnGa_2O_4$, g-C_3N_4	698 nm	RhB	99.2% in 100 min	42
ZGO-EDTA	—	MO	93.4% in 24 h	46
$SrAl_2O_4$:Eu^{2+}, Dy^{3+}, ZnO	494 nm	RhB	100% in 30 min	47
$SrAl_2O_4$:Eu^{2+}, Dy^{3+}, Ag	470 nm	RhB, MO, MB	88.9% in 24 h	48
$SrAl_2O_4$:Eu^{2+}, Dy^{3+}, Ag_3PO_4	460 nm	RhB	30% in 30 min	49
$CaAl_2O_4$:Eu^{2+}, Nd^{3+}, Ag_3PO_4	440 nm	RhB	81.7% in 5 h	50

also exhibited the highest removal effect after light irradiation was off. In the following year, they prepared a light-storing photocatalytic composite using melamine and g-C_3N_4 as precursors, matching $Sr_2MgSi_2O_7$:(Eu, Dy) emitting blue afterglow. It was observed that g-C_3N_4/$Sr_2MgSi_2O_7$:(Eu, Dy) with a ratio of 0.25 : 1 had the highest removal efficiency under 30 min illumination-140 min dark. This is the first time the interface model of g-C_3N_4/$Sr_2MgSi_2O_7$:(Eu, Dy) was constructed and analyzed by first-principles calculations. Fig. 4 shows the energy level of g-C_3N_4/$Sr_2MgSi_2O_7$:(Eu, Dy) and its possible mechanism. Their studies showed that the Eu 4f electrons have difficulty in returning to the Eu 5d orbitals after being captured by the C 2p orbitals, resulting in a decrease in light energy radiation. Also, the built-in electric field and energy band offsets between g-C_3N_4 and $Sr_2MgSi_2O_7$:(Eu, Dy) interreact with each other to promote the transfer of photoinduced carriers, which follows a traditional type-II transfer model, resulting in enhanced photocatalytic activity and decreased luminescence afterglow performance.

In their studies, they constructed a novel system of light-storing-assisted photocatalytic composite, which coupled a long afterglow material and photocatalyst, and the photocatalytic performance of the photocatalytic composite is due to the synergistic effects between the electric field and energy band offsets. Thus, they provided a reference for designing and optimizing the photocatalytic structure, which was verified by first-principles calculations, and the carrier transfer at the photocatalytic composite interface was beneficial for the characterization of the photocatalytic composite.

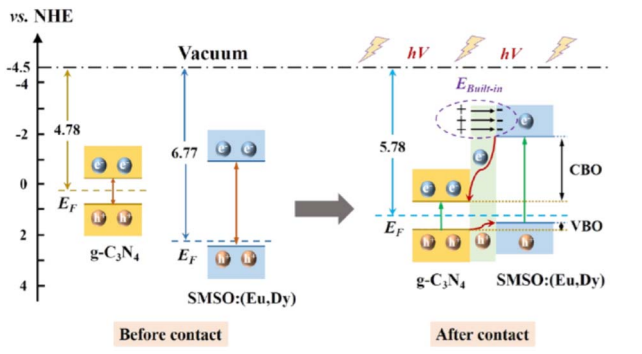

Fig. 4 Energy band arrangements and the transfer paths of carriers. (Reproduced from ref. 60 with permission from Elsevier, Copyright 2022.)

3.3 Energy reproduction

Although fossil energy increases the emission of greenhouse gas and other poisonous gases, it is still the most suitable to satisfy the essential requirement of energy. Consequently, from the perspective of environmental protection, sustainable development scenarios for finding clean energy and technology of waste-to-energy are key research interests.[61,62] In this case, hydrogen with a high energy density will furnish an inexhaustible energy source, but its safe storage and transportation are limiting factors in its commercial application due to its flammable and explosive characteristics. Present hydrogen production mainly involves the use of fossil fuels but water electrolysis[63,64] has emerged as an alternative.[65]

Cui *et al.* reported that $Sr_2MgSi_2O_7$:Eu^{2+}, Dy^{3+}, a micrometer-sized LAL material, can store and release energy after illumination, which was synthesized *via* the sol–gel method. This special LAL material exhibited an outstanding hydrogen production conversion efficiency for reforming methanol and water under round-the clock conditions, obtaining 5.18% solar-to-hydrogen conversion efficiency in the photocatalytic system.[66] The specific carrier transport path and abundant lattice defects were the foundation of the photocatalytic process. The long-lived carriers are an efficient way to improve photocatalytic activity. Also, it should be noted that this LAL material exhibited the highest STH conversion efficiency in the reported photocatalytic systems. This finding provides a tactic to construct efficient photocatalysts, which can extend the carrier lifetime.

The excess CO_2 from the consumption of fossil fuels to date has caused serious global climate change and energy crisis. Thus, the abundant CO_2 feedstock has driven researchers to achieve CO_2 chemical utilization.[67] Accordingly, CO_2 conversion using sunlight-driven photocatalysts is a crucial technique for closing the carbon cycle; however, intermittent solar flux is the bottleneck of catalysis. Thus, to address this, Pei *et al.* successfully synthesized oxygen-deficient Vo-SMSED, possessing electron transfer paths and active sites. The LAL Vo-SMSED material exhibited near 100% conversion in catalyzing CO_2

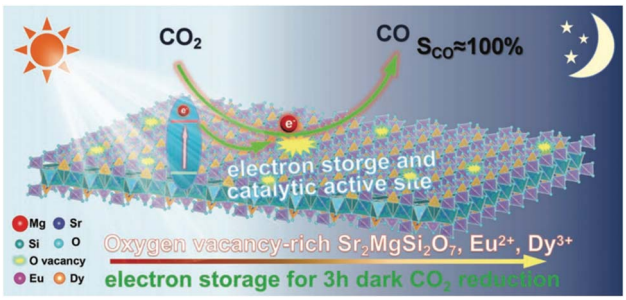

Fig. 5 Scheme for the photoreduction of CO_2 into CO on Vo-SMSED in the light and dark. (Reproduced from ref. 67 with permission from Wiley-VCH, Copyright 2022.)

reduction to CO at a speed of 1.15 μmol g^{-1} h^{-1} in the absence of illumination within 3 h because of the increasing electron transfer paths and active sites by Vo. Fig. 5 shows the proposed energy storage process and mechanism of the Vo-SMSED catalyst. In the literature, authors indicated that Vo is significant to activate the SMSED material for CO production around-the-clock, where the CO production on Vo-SMSED is roughly twice that of the pristine SMSED. This work provides a novel candidate method for the efficient and continuous photoreduction of CO_2 in the future.

4 Conclusions and perspectives

LAL materials can act as an inner excitation source in the photocatalytic process without external light, given that can release stored energy to excite the activity of photocatalysts in the dark. Thus, LAL materials provide a feasible system to maintain persistent intensity to support the function of photocatalysts, innovating a new idea to alleviate the energy crisis and environmental pollution. In recent years, lots of reviews have been reported on the application of persistent materials, but the photocatalytic field remains vague.

In this review, with the aim of understanding the role of LAL materials in photocatalysis, we compiled the mechanism of LAL materials firstly. We presented the recent progress of the LAL materials applied in photocatalytic reactions, disclosing their photocatalytic efficiency for the degradation of dyes and removal of poisonous gases, even illustrating H_2 production and CO_2 conversion using LAL materials to alleviate the energy crisis.

All studies are conducted in the laboratory, but practical applications are important. Considering the fact that LAL materials have self-luminous superiority, they have potential for full-scale applications in the future. However, presently, afterglow-catalytic systems face several challenging issues, as follows: (1) the photocatalytic efficiency is low under visible light and the duration time of charge storage is less than 1 hour; (2) many afterglow-catalytic systems commonly consist of interfaced photocatalyst and charge storage materials; however, the carrier transfer between heterogeneous composites with different band gaps must overcome the high interface energy barrier; (3) the recombination luminescence of carriers in the competition of movement often causes photocatalyst poisoning; and (4) the spatial separation of electron–hole pairs is different, and thus it is necessary to use hole-scavenging species.

For practical applications, heterojunction construction, surface modification, and defect engineering can be adopted to prolong the duration time of charge storage, and core@shell structures can be synthesised for resolving the poisoning issue of photocatalysts. As highlighted in this review, we hope that this topic will attract significant attention from scientists, solving the current environmental problems and realizing waste-to-energy, which is of great significance for forthcoming photocatalytic investigations. The potential challenges can be addressed employing the adjustable properties of combinations of LAL materials and photocatalysts, making composites meet the requirements. Further works should not be limited to the degradation of dyes; more importantly, changing waste into treasure such as CO_2 chemical utilization.

Author contributions

Yuxin Guo: conceptualization, writing-original draft, supervision, funding acquisition. Qiuwen Wang: formal analysis, writing-review and editing. Siyu Liu: formal analysis. Wen Ya: formal analysis. Ping Qi: writing-review and editing. Zenan Ni: conceptualization, writing-review and editing, supervision, funding acquisition. Huimin Liu: writing-review and editing. Qijian Zhang: writing-review and editing.

Conflicts of interest

All authors declare no conflict of interest.

Acknowledgements

This work was supported by the Foundation of Liaoning Province Education Department of China (LJKQZ20222297), Foundation of Liaoning Province Education Department of China (LJKMZ20220982), and Liaoning Province Applied Basic Research program (2022JH2/101300125).

References

1 L. Xiao, J. Liu and J. Ge, *Agr. Water Manage.*, 2021, **243**, 106417–106425.
2 F. Chen and Z. Chen, *Sci. Total Environ.*, 2021, **755**, 142543–142556.
3 E. Romero, V. I. Novoderezhkin and R. van Grondelle, *Nature*, 2017, **543**, 355–365.
4 H. He, Z. Luo and C. Yu, *J. Alloys Compd.*, 2020, **816**, 152652.
5 H. He, Z. Luo, Z.-Y. Tang and C. Yu, *Appl. Surf. Sci.*, 2019, **490**, 460–468.
6 H. He, J. Li, C. Yu and Z. Luo, *Sustainable Mater. Technol.*, 2019, **22**, e00127.
7 Z. Liu, J. Tian, C. Yu, Q. Fan and X. Liu, *Chin. J. Catal.*, 2022, **43**, 472–484.

8 P. Pattnaik, G. S. Dangayach and A. K. Bhardwaj, *Rev. Environ. Health*, 2018, **33**, 163–203.
9 D. Bidwai, N. K. Sahu and G. Swati, *Nanostructured Materials for Visible Light Photocatalysis*, Elsevier, 2022, pp. 251-275.
10 Y. H. Zhao, J. T. Geng, J. C. Cai, Y. F. Cai and C. Y. Cao, *Adsorpt. Sci. Technol.*, 2020, **38**, 151–167.
11 T. K. Vo, *Environ. Sci. Pollut. Res. Int.*, 2022, **29**, 42991–43003.
12 J. Zhou, J. Ding, H. Wan and G. Guan, *J. Colloid Interface Sci.*, 2021, **582**, 961–968.
13 H. L. Nguyen, *Adv. Energy Mater.*, 2020, **10**, 2002091–2002113.
14 H. N. Wang, Y. H. Zou, H. X. Sun, Y. Chen, S. L. Li and Y. Q. Lan, *Coord. Chem. Rev.*, 2021, **438**, 213906–213947.
15 D. Bidwai, N. Kumar Sahu, S. J. Dhoble, A. Mahajan, D. Haranath and G. Swati, *Methods Appl. Fluoresc.*, 2022, **10**, 032001–032031.
16 J. Wu, W. Zheng and Y. Chen, *Curr. Opin. Green Sustainable Chem.*, 2022, **33**, 100580–100585.
17 S. Gaoming, S. Ruichen, T. Jie and Q. Yuan, *Chem. J. Chin. Univ.*, 2020, **41**, 2404–2414.
18 Y. Li, M. Gecevicius and J. Qiu, *Chem. Soc. Rev.*, 2016, **45**, 2090–2136.
19 F. Kang, G. Sun, P. Boutinaud, H. Wu, F. X. Ma, J. Lu, J. Gan, H. Bian, F. Gao and S. Xiao, *Chem. Eng. J.*, 2021, **403**, 126099–126141.
20 J. Xu and S. Tanabe, *J. Lumin.*, 2019, **205**, 581–620.
21 J. Y. Y. Loh, N. P. Kherani and G. A. Ozin, *Nat. Sustain.*, 2021, **4**, 466–473.
22 Y. Zhang, Z. W. Wang, X. Ji, T. Wang, X. T. Yang and H. F. Wang, *J. Phys. Chem.*, 2021, **125**, 9096–9106.
23 K. Van den Eeckhout, P. F. Smet and D. Poelman, *Materials*, 2010, **3**, 2536–2566.
24 H. F. Brito, J. Hls, T. Laamanen, M. Lastusaari and L. C. V. Rodrigues, *Opt. Mater. Express*, 2012, **2**, 371–381.
25 Z. Ma, S. Liu, L. Pei and J. Zhong, *Lasers Optoelectron.*, 2021, **58**, 54–66.
26 T. Nakamura, K. Kaiya, N. Takahashi, T. Matsuzawa, C. C. Rowlands, V. Beltran-Lopez, G. M. Smith and P. C. Riedi, *J. Mater. Chem.*, 2000, **10**, 2566–2569.
27 T. Aitasalo, P. Dereń, J. Hölsä, H. Jungner, J. C. Krupa, M. Lastusaari, J. Legendziewicz, J. Niittykoski and W. Stręk, *J. Solid State Chem.*, 2003, **171**, 114–122.
28 J. Hölsä, T. Aitasalo, H. Jungner, M. Lastusaari, J. Niittykoski and G. Spano, *J. Alloys Compd.*, 2004, **374**, 56–59.
29 P. Dorenbos, *J. Lumin.*, 2003, **104**, 239–260.
30 P. Dorenbos, *J. Lumin.*, 2005, **111**, 89–104.
31 Z. Liang, C.-F. Yan, S. Rtimi and J. Bandara, *Appl. Catal., B*, 2019, **241**, 256–269.
32 Y. Zhang, K. Hawboldt, L. Zhang, J. Lu, L. Chang and A. Dwyer, *Appl. Catal., A*, 2022, **630**, 118460–118474.
33 A. Ahmad, S. H. Mohd-Setapar, C. S. Chuong, A. Khatoon, W. A. Wani, R. Kumar and M. Rafatullah, *RSC Adv.*, 2015, **5**, 30801–30818.
34 S. Natarajan, H. C. Bajaj and R. J. Tayade, *J. Environ. Sci.*, 2018, **65**, 201–222.
35 J. M. Fan, Z. H. Zhao, C. Gong, Y. Q. Xue and S. Yin, *J. Nanosci. Nanotechnol.*, 2018, **18**, 1675–1681.
36 V. Vaiano, O. Sacco and D. Sannino, *J. Cleaner Prod.*, 2019, **210**, 1015–1021.
37 X. Ma, J. Zhang, H. Li, B. Duan, L. Guo, M. Que and Y. Wang, *J. Alloys Compd.*, 2013, **580**, 564–569.
38 C. Zhou, P. Zhan, J. Zhao, X. Tang, W. Liu, M. Jin and X. Wang, *Ceram. Int.*, 2020, **46**, 27884–27891.
39 C. Yang, F. Zhang, X. Liu, Y. Du, D. Huang, J. Liu, L. Xie, G. Zhou and J. Tang, *J. Solid State Chem.*, 2022, **310**, 123057–123064.
40 S. S. Li, M. Liu, L. Wen, Z. Xu, Y. H. Cheng and M. L. Chen, *Environ. Sci. Pollut. Res. Int.*, 2023, **30**, 322–336.
41 K. Hong, J. Hong and Y. Kim, *J. Photochem. Photobiol., A*, 2020, **396**, 112520–112528.
42 A. Tuerdi and A. Abdukayum, *RSC Adv.*, 2019, **9**, 17653–17657.
43 D. Li, Y. Wang, K. Xu, H. Zhao and Z. Hu, *RSC Adv.*, 2015, **5**, 20972–20975.
44 Y. E. Lee, D. P. Norton, C. Park and C. M. Rouleau, *J. Appl. Phys.*, 2001, **89**, 1653–1657.
45 S. C. Yan, S. X. Ouyang, J. Gao, M. Yang, J. Y. Feng, X. X. Fan, L. J. Wan, Z. S. Li, J. H. Ye, Y. Zhou and Z. G. Zou, *Angew. Chem., Int. Ed. Engl.*, 2010, **49**, 6400–6404.
46 S. G. Menon, A. K. Bedyal, T. Pathak, V. Kumar and H. C. Swart, *J. Alloys Compd.*, 2021, **860**, 158370–158378.
47 O. Hai, M. Pei, E. Yang, Q. Ren, X. Wu, J. Zhu, Y. Zhao and L. Du, *J. Alloys Compd.*, 2021, **866**, 158752–158759.
48 Y. Wang, S. Wu, D. Li, W. Lei, Y. Shen and F. Li, *J. Mater. Sci.*, 2022, **57**, 14877–14889.
49 M. Zhang, F. Li, S. Jiang, Y. C. Lin, F. Chen, X. Zhao and Y. Shen, *Opt. Mater.*, 2021, **116**, 111049–111056.
50 M. Jakob, H. Levanon and P. V. Kamat, *Nano Lett.*, 2003, **3**, 353–358.
51 L. Zhang, Q. Zhang, H. Xie, J. Guo, H. Lyu, Y. Li, Z. Sun, H. Wang and Z. Guo, *Appl. Catal., B*, 2017, **201**, 470–478.
52 Z. Li, Y. Wei, H. Cui, G. Jiang and Z. Guo, *J. Electrochem. Soc.*, 2017, **164**, H651–H656.
53 L. Zhang, X. Li, S. Chen, J. Guan, Y. Guo and W. Yu, *Catal. Commun.*, 2023, **176**, 106627.
54 Y. H. Chiu and Y. J. Hsu, *Nano Energy*, 2017, **31**, 286–295.
55 M. Y. Kuo, C. F. Hsiao, Y. H. Chiu, T. H. Lai, M. J. Fang, J. Y. Wu, J. W. Chen, C. L. Wu, K. H. Wei, H. C. Lin and Y. J. Hsu, *Appl. Catal., B*, 2019, **242**, 499–506.
56 J. Fragoso, A. Pastor, M. Cruz-Yusta, F. Martin, G. de Miguel, I. Pavlovic, M. Sánchez and L. Sánchez, *Appl. Catal., B*, 2023, **322**, 122115–122126.
57 C. Hu, W. F. Tsai, W. H. Wei, K. Y. Andrew Lin, M. T. Liu and K. Nakagawa, *Carbon*, 2021, **175**, 467–477.
58 D. Huang, Z. Li, G. Zeng, C. Zhou, W. Xue, X. Gong, X. Yan, S. Chen, W. Wang and M. Cheng, *Appl. Catal., B*, 2019, **240**, 153–173.
59 Q. Zhou, F. Peng, Y. Ni, J. Kou, C. Lu and Z. Xu, *J. Photochem. Photobiol., A*, 2016, **328**, 182–188.
60 X. Yang, B. Tang and X. Cao, *J. Environ. Chem. Eng.*, 2022, **10**, 108820.
61 A. Midilli, M. Ay, I. Dincer and M. A. Rosen, *Renewable Sustainable Energy Rev.*, 2005, **9**, 273–287.

62 X. Chen, S. Shen, L. Guo and S. Mao, *Chem. Rev.*, 2010, **110**, 6503–6570.
63 Y. Zhang, K. Hawboldt, L. Zhang, J. Lu, L. Chang and A. Dwyer, *Appl. Catal., A*, 2022, **630**, 118460.
64 K. Zeng and D. Zhang, *Prog. Energy Combust. Sci.*, 2010, **36**, 307–326.
65 S. Dutta, *J. Ind. Eng. Chem.*, 2014, **20**, 1148–1156.
66 G. Cui, X. Yang, Y. Zhang, Y. Fan, P. Chen, H. Cui, Y. Liu, X. Shi, Q. Shang and B. Tang, *Angew. Chem., Int. Ed.*, 2019, **58**, 1340–1344.
67 L. Pei, Z. Ma, J. Zhong, W. Li, X. Wen, J. Guo, P. Liu, Z. Zhang, Q. Mao, J. Zhang, S. Yan and Z. Zou, *Adv. Funct. Mater.*, 2022, **32**, 2208565–2208574.